

1 **Supporting Information for**2 **ORIGINAL ARTICLE**3 **Silybin A from *Silybum marianum* reprograms lipid metabolism to induce a**
4 **cell fate-dependent class switch from triglycerides to phospholipids**

5

6 Solveigh C. Koeberle^{a,b,†,*}, Maria Thürmer^{c,†}, [Fengting Su^{a,b}](#), Markus Werner^c, Julia Grandner^b,7 Laura Hofer^b, André Gollowitzer^b, Loc Le Xuan^b, Felix J. Benschaid^b, Ehsan Bonyadi Rad^b,8 Armando Zarrelli^d, Giovanni Di Fabio^d, Oliver Werz^e, Valeria Romanucci^d, Amelie Lupp^e,9 Andreas Koeberle^{a,b,e,*}10 [* Corresponding authors: Andreas Koeberle, University of Graz, Graz, 8010, Austria.](#)11 [Solveigh C. Koeberle, University of Graz, Graz, 8010, Austria.](#)

12

13 ^a[Institute of Pharmaceutical Sciences/Pharmacognosy University of Graz, 8010 Graz, Austria](#)14 ^b[Michael Popp Institute and Center for Molecular Biosciences Innsbruck \(CMBI\), University](#)
15 [of Innsbruck, 6020 Innsbruck, Austria](#)16 ^c[Department of Pharmaceutical/Medicinal Chemistry, Institute of Pharmacy, Friedrich](#)
17 [Schiller University Jena, 07743 Jena, Germany](#)18 ^d[Department of Chemical Sciences, University of Napoli Federico II, Naples, Italy](#)19 ^e[Institute of Pharmacology and Toxicology, Jena University Hospital, Jena, Germany](#)

20

21

22 [*Corresponding authors. +43 316 380 - 8630.](#)23 [E-mail addresses: andreas.koeberle@uni-graz.at \(Andreas Koeberle\).](#)24 [solveigh.koeberle@uni-graz.at \(Solveigh Koeberle\).](#)

25

hat gelöscht: ^bhat gelöscht: ^bhat gelöscht: ^ahat gelöscht: ^ahat gelöscht: ^ahat gelöscht: Fengting Su^a,hat gelöscht: ^ahat gelöscht: ^ahat gelöscht: ^ahat gelöscht: ^ahat gelöscht: ^ahat gelöscht: ^bhat gelöscht: ^ahat gelöscht: ^a Corresponding authors: Andreas Koeberle,
Michael Popp Institute and Center for Molecular Biosciences
Innsbruck (CMBI), University of Innsbruck, Innsbruck, 6020,
Austria.¶
Solveigh C. Koeberle, Michael Popp Institute and Center for
Molecular Biosciences Innsbruck (CMBI), University of Innsbruck,
Innsbruck, 6020, Austria.¶hat gelöscht: ^a

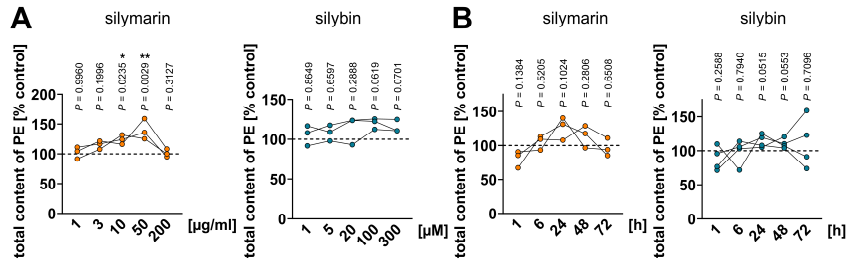
hat gelöscht: ¶

hat gelöscht: ^bhat gelöscht: ^ahat gelöscht: ^a

52 **Supplementary Figures**

53

54



55

56 Figure S1. Concentration- and time-dependent effects of silymarin and silybin on cellular PE levels.

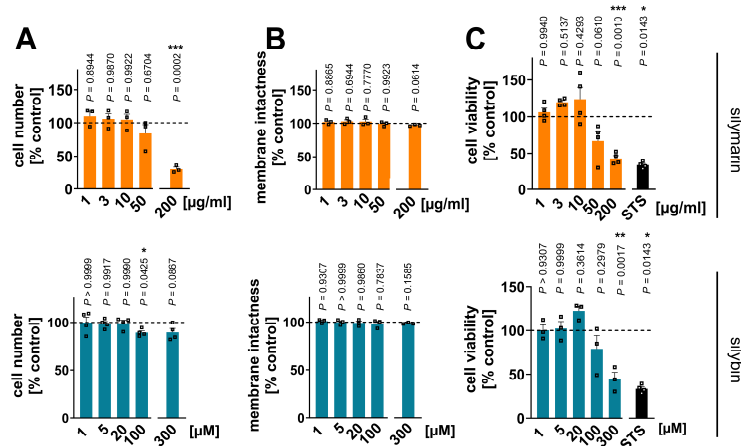
57 (A, B) HepG2 cells were treated with silymarin, silybin or vehicle (ethanol for silymarin, DMSO for

58 silybin) at the indicated concentrations for 24 h (A) or with silymarin (10 $\mu\text{g/ml}$), silybin (20 μM) or

59 vehicle (ethanol for silymarin, DMSO for silybin) for the indicated incubation times (B). Independent

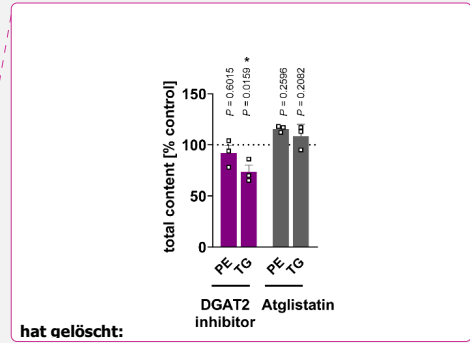
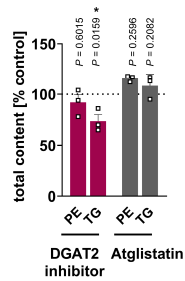
60 datasets connected by lines; $n = 3$ (A, B, silymarin) or $n = 4$ (B, silybin). * $P < 0.05$, ** $P < 0.01$ vs.61 vehicle control for the respective time point; two-tailed paired Student's t -test.

62



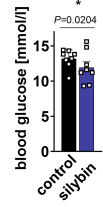
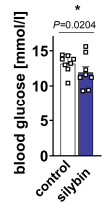
63

64 Figure S2. Effects of silymarin and silybin on cell number, membrane integrity and cell viability.
 65 HepG2 cells were treated with silymarin and silybin (at the indicated concentrations), staurosporine
 66 (STS, 1 µM) (C), or vehicle (ethanol for silymarin, DMSO for silybin and STS) for 24 h. (A) Cell
 67 numbers. Individual values and mean + SEM; n = 3 (silymarin), or n = 4 (silybin). (B) Membrane
 68 intactness measured by trypan blue staining. Individual values and mean + SEM; n = 3; effects of
 69 silymarin (200 µg/ml) and silybin (300 µM) were assessed in independent experiments (A, B). (C)
 70 Cell viability determined by MTT assay. Individual values and mean + SEM; n = 3 (silybin) or n = 4
 71 (silymarin and STS). * $P < 0.05$, ** $P < 0.01$, *** $P < 0.001$ vs. vehicle control; ordinary one-way
 72 ANOVA + Tukey HSD *post hoc* tests (C) and two-tailed paired Student's *t*-test (A and B, 200 µg/ml
 73 silymarin and 300 µM silybin, C, STS).
 74



75

76 Figure S3. Influence of DGAT and ATGL inhibition on the phospholipid and TG content of
 77 hepatocytes. HepG2 cells were treated with the DGAT inhibitor PF 06424439 or the ATGL inhibitor
 78 atglistatin for 24-30 h. Total amounts of PE and TG were determined by UPLC-MS/MS. Individual
 79 values and mean + SEM; n = 3. * $P < 0.05$ vs. vehicle control; two-tailed unpaired Student's *t*-test.
 80



hat gelöscht:

82

83 Figure S4. Blood glucose levels. Mice received silybin hemisuccinate ('silybin'; 200 mg/kg, i.p.) or
84 vehicle (0.9% NaCl) trice at 0, 12, and 24 h and were sacrificed after 37 h. Individual values and mean
85 from n = 8 mice/group, * $P < 0.05$ vs. vehicle control; two-tailed unpaired Student's t -test.
86

87

88

A

monocytes

	PC			
	control	silymarin	control	silybin
PC(16:0_16:0)	1.217 ± 0.397	1.485 ± 0.345	0.972 ± 0.06	1.053 ± 0.062
PC(16:0_18:1)	0.681 ± 0.254	1.089 ± 0.276	0.456 ± 0.015	0.542 ± 0.019
PC(18:0_18:1)	0.303 ± 0.099	0.46 ± 0.06	1.804 ± 0.089	2.064 ± 0.116
PC(18:1_18:1)	0.329 ± 0.133	0.518 ± 0.152	0.374 ± 0.035	0.440 ± 0.035
PC(18:1_20:1)	0.053 ± 0.023	0.08 ± 0.02	0.081 ± 0.016	0.101 ± 0.016
PC(16:0_18:2)	0.098 ± 0.029	0.211 ± 0.034	0.178 ± 0.007	0.232 ± 0.01
PC(18:0_18:2)	0.106 ± 0.039	0.188 ± 0.017	0.51 ± 0.01	0.566 ± 0.029
PC(16:0_20:3)	0.045 ± 0.019	0.06 ± 0.028	0.038 ± 0.004	0.046 ± 0.004
PC(18:0_20:4)	0.094 ± 0.032	0.164 ± 0.039	0.232 ± 0.008	0.248 ± 0.006
PC(18:1_20:4)	0.037 ± 0.012	0.064 ± 0.013	0.093 ± 0.003	0.105 ± 0.004
PC(18:0_20:3)	0.011 ± 0.004	0.017 ± 0.005	0.019 ± 0.002	0.048 ± 0.021
PC(18:0_20:4)	0.012 ± 0.003	0.034 ± 0.004	0.028 ± 0.001	0.024 ± 0.000
PC(16:0_22:5)	0.291 ± 0.078	0.347 ± 0.073	0.213 ± 0.025	0.228 ± 0.022
PC(18:0_22:6)	0.058 ± 0.016	0.078 ± 0.006	0.021 ± 0.002	0.021 ± 0
PC 32:0 E (16:0)	0.02 ± 0.008	0.023 ± 0.001	0.183 ± 0.02	0.182 ± 0.017
PC 34:2 E (18:2)	0.128 ± 0.047	0.197 ± 0.046	0.255 ± 0.013	0.257 ± 0.009

	PE			
	control	silymarin	control	silybin
PE(16:0_18:1)	0.057 ± 0.02	0.102 ± 0.031	0.148 ± 0.019	0.24 ± 0.031
PE(18:0_18:1)	0.693 ± 0.289	0.978 ± 0.28	1.261 ± 0.067	1.323 ± 0.035
PE(18:1_18:1)	0.156 ± 0.058	0.263 ± 0.087	0.204 ± 0.024	0.322 ± 0.045
PE(18:1_20:1)	0.039 ± 0.017	0.079 ± 0.03	0.029 ± 0.002	0.035 ± 0.003
PE(18:0_20:4)	0.483 ± 0.174	0.756 ± 0.206	1.781 ± 0.112	2.134 ± 0.142
PE(18:0_22:5)	0.046 ± 0.02	0.069 ± 0.022	0.129 ± 0.007	0.145 ± 0.008
PE 34:1 E (16:0)	0.158 ± 0.051	0.193 ± 0.053	0.247 ± 0.032	0.281 ± 0.026

B

HepG2

	PC			
	control	silymarin	control	silybin
PC(16:0_16:0)	0.762 ± 0.058	0.943 ± 0.057	0.714 ± 0.083	0.778 ± 0.079
PC(16:0_18:1)	1.369 ± 0.125	2.123 ± 0.056	1.082 ± 0.164	1.257 ± 0.173
PC(16:0_18:1)	1.377 ± 0.746	4.94 ± 0.133	1.97 ± 0.414	3.486 ± 0.441
PC(18:1_18:1)	2.149 ± 0.17	3.275 ± 0.048	2.493 ± 0.264	3.03 ± 0.194
PC(16:0_18:2)	0.451 ± 0.044	0.688 ± 0.024	0.47 ± 0.063	0.523 ± 0.052

	PE			
	control	silymarin	control	silybin
PE(16:0_16:1)	0.155 ± 0.013	0.255 ± 0.011	0.196 ± 0.01	0.228 ± 0.003
PE(16:0_18:1)	0.67 ± 0.069	1.129 ± 0.044	1.545 ± 0.764	1.85 ± 0.831
PE(18:0_18:1)	1.029 ± 0.128	1.735 ± 0.11	4.748 ± 1.2	6.695 ± 1.636
PE(18:1_18:1)	1.022 ± 0.089	1.588 ± 0.111	1.10 ± 0.219	1.469 ± 0.195
PE(18:0_20:4)	0.74 ± 0.086	1.036 ± 0.045	1.020 ± 0.231	1.259 ± 0.246

	PS			
	control	silymarin	control	silybin
PS(16:0_18:1)	0.116 ± 0.015	0.147 ± 0.01	0.109 ± 0.009	0.117 ± 0.009
PS(18:0_18:1)	0.132 ± 0.014	0.187 ± 0.008	0.672 ± 0.072	0.822 ± 0.291
PS(18:1_18:1)	0.806 ± 0.292	1.056 ± 0.053	0.158 ± 0.01	0.173 ± 0.014
PS(18:0_18:2)	0.09 ± 0.01	0.122 ± 0.009	0.103 ± 0.015	0.111 ± 0.011

	PI			
	control	silymarin	control	silybin
PI(16:0_18:1)	0.206 ± 0.013	0.316 ± 0.016	0.159 ± 0.015	0.18 ± 0.024
PI(18:1_18:1)	0.228 ± 0.014	0.383 ± 0.011	0.207 ± 0.03	0.252 ± 0.044
PI(16:0_20:4)	0.046 ± 0.004	0.059 ± 0.002	0.054 ± 0.0021	0.039 ± 0.006
PI(18:0_20:4)	0.31 ± 0.034	0.415 ± 0.009	0.195 ± 0.027	0.193 ± 0.036

	PG			
	control	silymarin	control	silybin
PG(16:1_18:1)	0.138 ± 0.001	0.176 ± 0.015	0.148 ± 0.02	0.167 ± 0.024
PG(18:0_18:1)	0.133 ± 0.006	0.149 ± 0.006	0.238 ± 0.034	0.248 ± 0.053
PG(18:1_18:1)	0.055 ± 0.002	0.081 ± 0.001	0.075 ± 0.011	0.106 ± 0.022

PS

PI

PG

SM

TG

SM

TG

SM

TG

PS

PI

PG

SM

TG

SM

TG

SM

TG

SM

TG

SM

TG

SM

TG

SM

TG

SM

TG

SM

TG

SM

TG

SM

TG



A

monocytes

	PC			
	control	silymarin	control	silybin
PC(16:0_16:0)	1.217 ± 0.397	1.485 ± 0.345	0.972 ± 0.06	1.053 ± 0.062
PC(16:0_18:1)	0.681 ± 0.254	1.089 ± 0.276	0.456 ± 0.015	0.542 ± 0.019
PC(18:0_18:1)	0.303 ± 0.099	0.46 ± 0.06	1.804 ± 0.089	2.064 ± 0.116
PC(18:1_18:1)	0.329 ± 0.133	0.518 ± 0.152	0.374 ± 0.035	0.440 ± 0.035
PC(18:1_20:1)	0.053 ± 0.023	0.08 ± 0.02	0.081 ± 0.016	0.101 ± 0.016
PC(16:0_18:2)	0.098 ± 0.029	0.211 ± 0.034	0.178 ± 0.007	0.232 ± 0.01
PC(18:0_18:2)	0.106 ± 0.039	0.188 ± 0.017	0.51 ± 0.01	0.566 ± 0.029
PC(16:0_20:3)	0.045 ± 0.019	0.06 ± 0.028	0.038 ± 0.004	0.046 ± 0.004
PC(18:0_20:4)	0.094 ± 0.032	0.164 ± 0.039	0.232 ± 0.008	0.248 ± 0.006
PC(18:1_20:4)	0.037 ± 0.012	0.064 ± 0.013	0.093 ± 0.003	0.105 ± 0.004
PC(18:0_20:3)	0.011 ± 0.004	0.017 ± 0.005	0.019 ± 0.002	0.048 ± 0.021
PC(18:0_20:4)	0.012 ± 0.003	0.034 ± 0.004	0.028 ± 0.001	0.024 ± 0.000
PC(16:0_22:5)	0.291 ± 0.078	0.347 ± 0.073	0.213 ± 0.025	0.228 ± 0.022
PC(18:0_22:6)	0.058 ± 0.016	0.078 ± 0.006	0.021 ± 0.002	0.021 ± 0.000
PC 32:0 E (16:0)	0.02 ± 0.008	0.023 ± 0.001	0.183 ± 0.02	0.182 ± 0.017
PC 34:2 E (18:2)	0.128 ± 0.047	0.197 ± 0.046	0.255 ± 0.013	0.257 ± 0.009

	PE			
	control	silymarin	control	silybin
PE(16:0_18:1)	0.057 ± 0.02	0.102 ± 0.031	0.148 ± 0.019	0.24 ± 0.031
PE(18:0_18:1)	0.693 ± 0.289	0.978 ± 0.28	1.261 ± 0.067	1.323 ± 0.035
PE(18:1_18:1)	0.156 ± 0.058	0.263 ± 0.087	0.204 ± 0.024	0.322 ± 0.045
PE(18:1_20:1)	0.039 ± 0.017	0.079 ± 0.03	0.029 ± 0.002	0.035 ± 0.003
PE(18:0_20:4)	0.483 ± 0.174	0.756 ± 0.206	1.781 ± 0.112	2.134 ± 0.142
PE(18:0_22:5)	0.046 ± 0.02	0.069 ± 0.022	0.129 ± 0.007	0.145 ± 0.008
PE 34:1 E (16:0)	0.158 ± 0.051	0.193 ± 0.053	0.247 ± 0.032	0.281 ± 0.026

B

HepG2

	PC			
	control	silymarin	control	silybin
PC(16:0_16:0)	0.762 ± 0.058	0.943 ± 0.057	0.714 ± 0.083	0.778 ± 0.079
PC(16:0_18:1)	1.369 ± 0.125	2.123 ± 0.056	1.082 ± 0.164	1.257 ± 0.173
PC(16:0_18:1)	1.377 ± 0.746	4.94 ± 0.133	1.97 ± 0.414	3.486 ± 0.441
PC(18:1_18:1)	2.149 ± 0.17	3.275 ± 0.048	2.493 ± 0.264	3.03 ± 0.194
PC(16:0_18:2)	0.451 ± 0.044	0.688 ± 0.024	0.47 ± 0.063	0.523 ± 0.052

	PE			
	control	silymarin	control	silybin
PE(16:0_16:1)	0.155 ± 0.013	0.255 ± 0.011	0.196 ± 0.01	0.228 ± 0.003
PE(16:0_18:1)	0.67 ± 0.069	1.129 ± 0.044	1.545 ± 0.764	1.85 ± 0.831
PE(18:0_18:1)	1.029 ± 0.128	1.735 ± 0.11	4.748 ± 1.2	6.695 ± 1.636
PE(18:1_18:1)	1.022 ± 0.089	1.588 ± 0.111	1.10 ± 0.219	1.469 ± 0.195
PE(18:0_20:4)	0.74 ± 0.086	1.036 ± 0.045	1.020 ± 0.231	1.259 ± 0.246

	PS			
	control	silymarin	control	silybin
PS(16:0_18:1)	0.116 ± 0.015	0.147 ± 0.01	0.109 ± 0.009	0.117 ± 0.009
PS(18:0_18:1)	0.132 ± 0.014	0.187 ± 0.008	0.672 ± 0.072	0.822 ± 0.291
PS(18:1_18:1)	0.806 ± 0.292	1.056 ± 0.053	0.158 ± 0.01	0.173 ± 0.014
PS(18:0_18:2)	0.09 ± 0.01	0.122 ± 0.009	0.103 ± 0.015	0.111 ± 0.011

	PI			
	control	silymarin	control	silybin
PI(16:0_18:1)	0.206 ± 0.013	0.316 ± 0.016	0.159 ± 0.015	0.18 ± 0.024
PI(18:1_18:1)	0.228 ± 0.014	0.383 ± 0.011	0.207 ± 0.03	0.252 ± 0.044
PI(16:0_20:4)	0.046 ± 0.004	0.059 ± 0.002	0.054 ± 0.0021	0.039 ± 0.006
PI(18:0_20:4)	0.31 ± 0.034	0.415 ± 0.009	0.195 ± 0.027	0.193 ± 0.036

	PG			
	control	silymarin	control	silybin
PG(16:1_18:1)	0.138 ± 0.001	0.176 ± 0.015	0.148 ± 0.02	0.167 ± 0.024
PG(18:0_18:1)	0.133 ± 0.006	0.149 ± 0.006	0.238 ± 0.034	0.248 ± 0.053
PG(18:1_18:1)	0.055 ± 0.002	0.081 ± 0.001	0.075 ± 0.011	0.106 ± 0.022

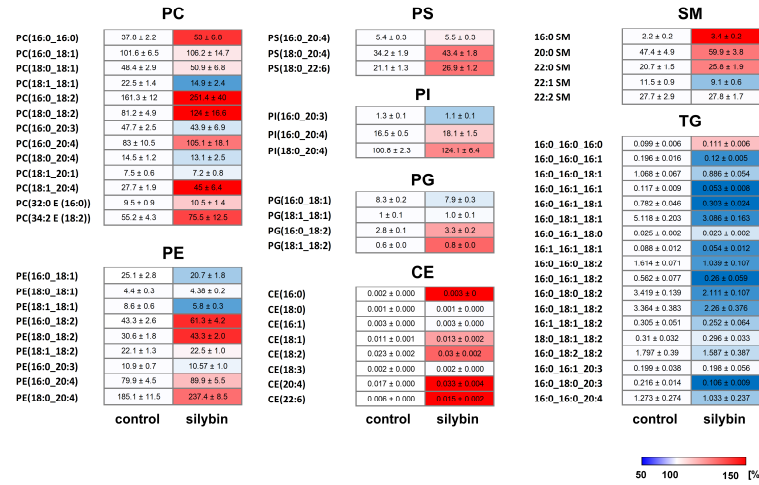
hat aelöscht:

A

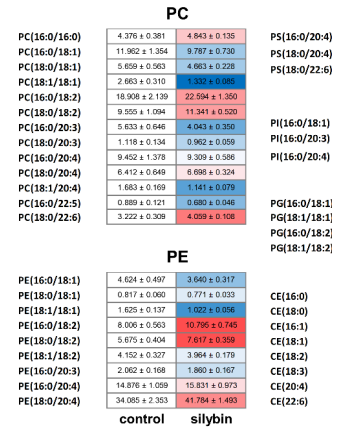
monocytes

	PC			
	control	silymarin	control	silybin
PC(16:0_16:0)	1.217 ± 0.397	1.485 ± 0.345	0.972 ± 0.06	1.053 ± 0.062
PC(16:0_18:1)	0.681 ± 0.254	1.089 ± 0.276	0.456 ± 0.015	0.542 ± 0.019
PC(18:0_18:1)	0.303 ± 0.099	0.46 ± 0.06	1.804 ± 0.089	2.064 ± 0.116
PC(18:1_18:1)	0.329 ± 0.133	0.518 ± 0.152	0.374 ± 0.035	0.440 ± 0.035
PC(18:1_20:1)	0.053 ± 0.023	0.08 ± 0.02	0.081 ± 0.016	0.101 ± 0.016
PC(16:0_18:2)	0.098 ± 0.029	0.211 ± 0.034	0.178 ± 0.007	0.232 ± 0.01
PC(18:0_18:2)	0.106 ± 0.039	0.188 ± 0.017	0.51 ± 0.01	0.566 ± 0.029
PC(16:0_20:3)	0.045 ± 0.019	0.06 ± 0.028	0.038 ± 0.004	0.046 ± 0.004
PC(18:0_20:4)	0.094 ± 0.032	0.164 ± 0.039	0.232 ± 0.008	0.248 ± 0.006
PC(18:1_20:4)	0.037 ± 0.012	0.064 ± 0.013	0.093 ± 0.003	0.105 ± 0.004
PC(18:0_20:3)	0.011 ± 0.004	0.017 ± 0.005	0.019	

mouse liver



mouse liver

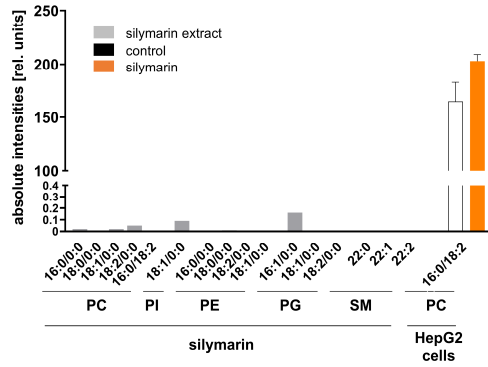


hat gelöscht:

hat gelöscht: normalized to the cell number (in relative units)

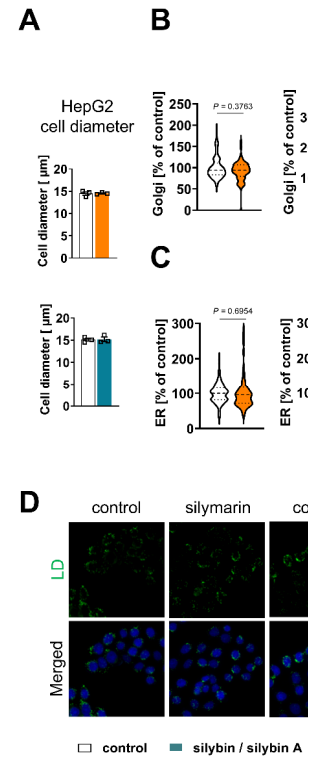
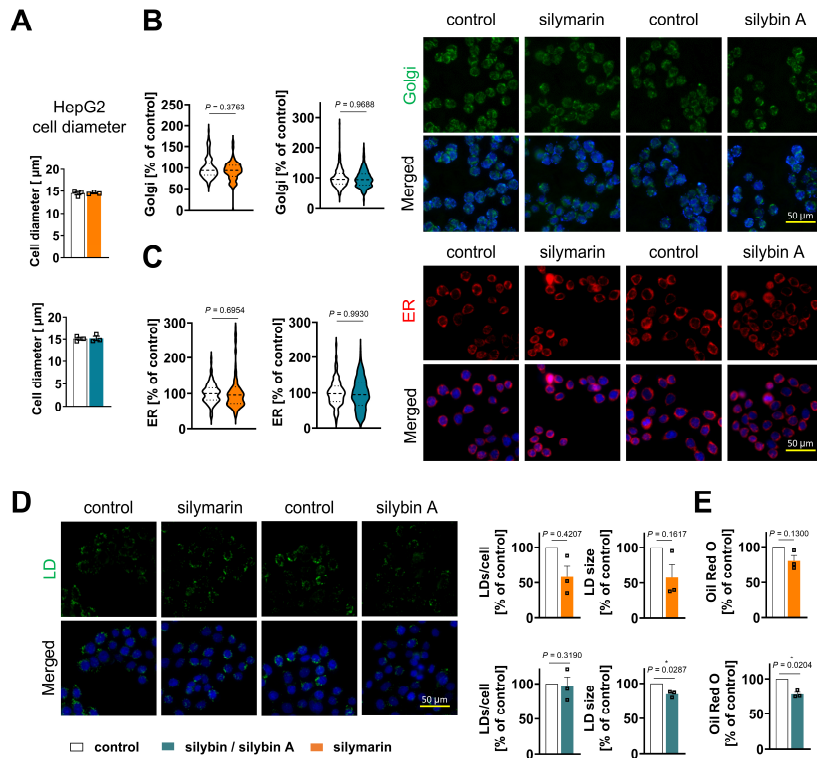
107
108
109
110
111
112
113

Figure S6. Phospholipid, TG and CE profile of mouse liver upon gavage of silybin. Mice were treated as described in Figure 1. Heatmap showing the absolute abundance of phospholipid, TG and CE species. Values are given as nmol for PC and units for PE, PS, PI, PG, SM and TG. Data are presented as mean ± SEM. The color indicates percentage changes relative to control. Data and the number of experiments are identical to Figure 1.

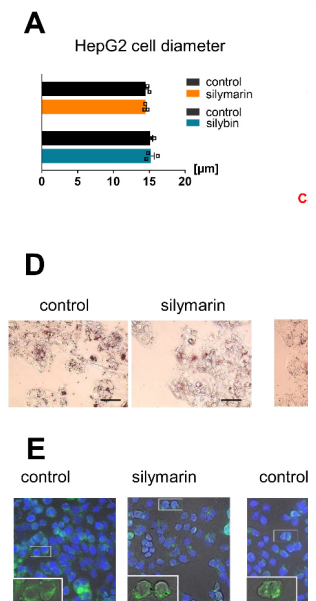


116

117 Figure S7. (Lyso)phospholipid content of silymarin in comparison to hepatocytes. Absolute abundance
 118 of (lyso)phospholipids in 10 μg silymarin or 3×10^5 HepG2 cells, which corresponds to the treatment
 119 of hepatocytes with 10 $\mu\text{g}/\text{ml}$ under our experimental conditions. Lipid analysis of HepG2 cells
 120 focused on those species from Figure S5 and S6 that are present in silymarin, i.e., PC(16:0/18:2).
 121 Single value or mean + SEM; n = 1 (silymarin) or n = 3 (HepG2 cells).
 122



hat gelöscht:



hat gelöscht:

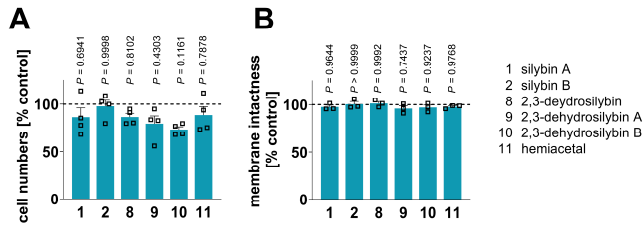
hat gelöscht: Impact on intracellular membrane compartments and lipid droplets. HepG2 cells were incubated with silymarin (10 $\mu\text{g/ml}$), silybin (20 μM) or vehicle control (ethanol for silymarin, DMSO for silybin) for 24 h. (A) Cell diameter (μm) of HepG2 cells determined with a Vi-CellTM XR cell counting system. Individual values and mean + SEM; $n = 3$. (B and C) Immunofluorescence staining of Golgi (B) and ER (C): anti-GM130 (red) was used as Golgi marker and anti-calnexin (red) as ER marker; nuclei were stained with DAPI (blue). (D) Left panel: Staining of lipid droplets with Oil Red O. Scale bar 50 μm . Right panel: Relative lipid droplet content. Individual values and mean + SEM; $n = 3$. $*P < 0.05$ vs. vehicle control. (E) Immunofluorescence staining of lipid droplets with BODIPY493/503 (green); nuclei were visualized with DAPI (blue). Lipid droplets were counted in three independent experiments for 100 cells (each). Images are representative out of 3 independent experiments; magnified BODIPY493/503-stained section: 40 \times 20 μm . Individual values and mean + SEM; $n = 3$. $*P < 0.05$ vs. vehicle control. Two-tailed paired Student's *t*-test (A, D, E).

123

124 **Figure S8. Impact of silymarin and silybin A on intracellular membrane compartments and lipid**
 125 **droplets. HepG2 cells were incubated with silymarin (10 $\mu\text{g/ml}$), silybin A (20 μM) or vehicle control**
 126 **(ethanol for silymarin, DMSO for silybin A) for 24 h. (A) Cell diameter of HepG2 cells determined**
 127 **with a Vi-CellTM XR cell counting system. Individual values and means + SEM; $n = 3$. (B-D) Labeling**
 128 **of Golgi with CellLightTM Golgi-GFP (B), ER with ER-TrackerTM TR (BODIPYTM TR**
 129 **Glibenclamide) (C) and lipid droplets with BioTrackerTM 488 Green Lipid Dye Biotracker (D); nuclei**
 130 **were stained with Hoechst 33342 (blue). Violine plots show quantification of the mean intensities for**
 131 **130 control cells (ethanol), 122 silymarin-treated cells, 551 control cells (DMSO), and 335 silybin A-**
 132 **treated cells (B); and for 127 control cells (ethanol), 131 silymarin-treated cells, 404 control cells**
 133 **(DMSO), and 366 silybin A-treated cells (C) from $n = 3$ independent experiments. Median and**
 134 **interquartile range are indicated as dotted lines. Quantification of the number and size of lipid droplets**
 135 **using the "Analyze Particles" tool in ImageJ for 103 control cells (ethanol), 126 silymarin-treated**
 136 **cells, 105 control cells (DMSO), and 120 silybin A-treated cells (D) from $n = 3$ independent**
 137 **experiments. The statistics were performed on the mean values of $n = 3$ independent experiments. (E)**
 138 **Relative lipid droplet content analyzed by Oil Red O staining. Individual values and mean + SEM; $n =$**
 139 **3. $*P < 0.05$ vs. vehicle control. Two-tailed paired Student's *t*-test on raw data (A, B, C, E). Scale bar**
 140 **50 μm .**

141

142

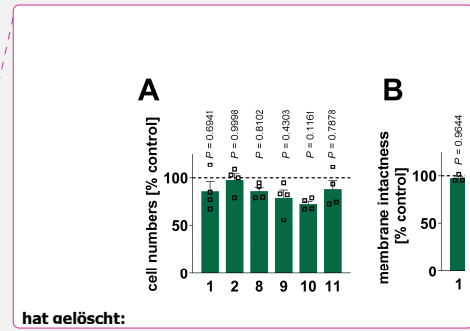


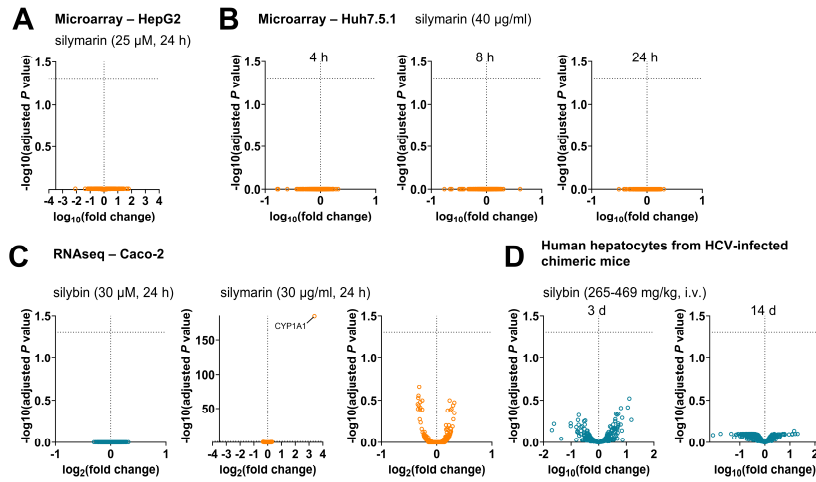
183

184 Figure S9. Effect of silybin derivatives on cell number and cell membrane intactness. HepG2 cells
 185 were treated with the indicated compounds (20 μ M) or vehicle (DMSO) for 24 h. (A) Cell numbers;
 186 (B) membrane intactness measured by trypan blue staining. Individual values and mean + SEM; n = 3
 187 (B) or n = 4 (A). P values vs. vehicle control; repeated measures one-way ANOVA + Tukey HSD *post*
 188 *hoc* tests.

189

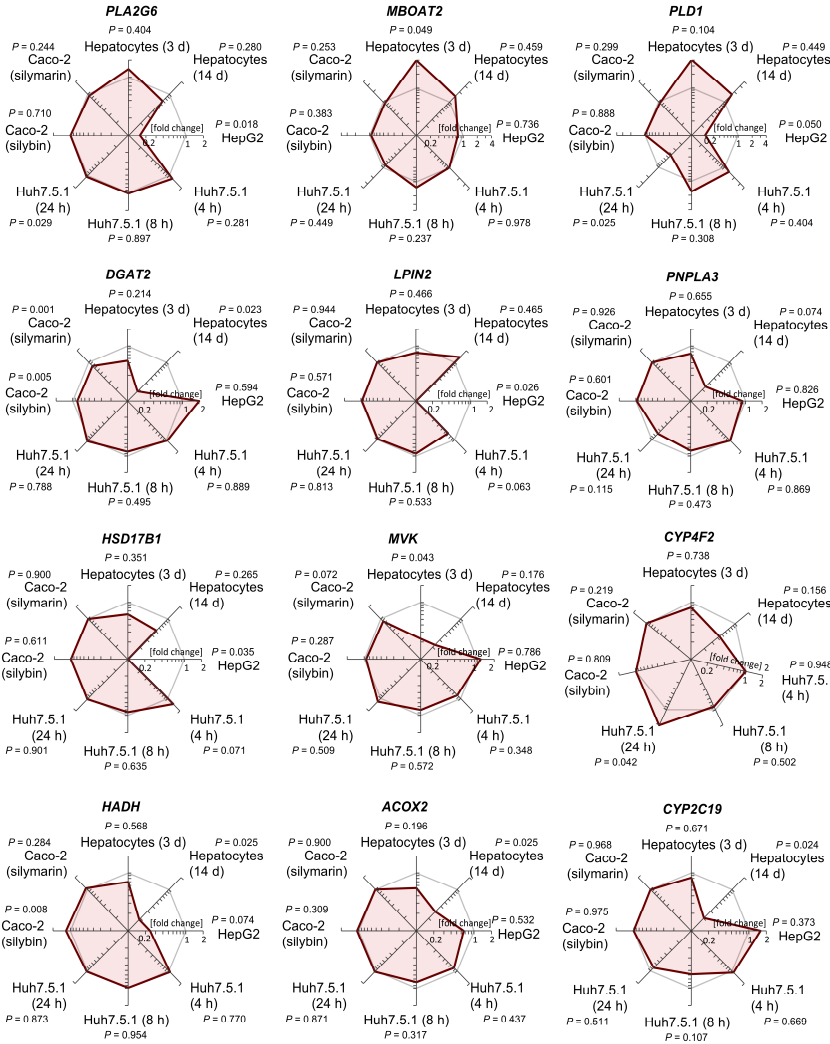
190





192

193 Figure S10. Volcano plots showing the data from Fig. 6A-D adjusted for multiple comparisons.
 194 Statistical calculations were performed by pairwise comparison of treatment and control groups using
 195 the GEO2R interactive webtool (<https://www.ncbi.nlm.nih.gov/geo/geo2r/>)¹.
 196 Adjusted *P* values were calculated by multiple *t*-tests, with correction for multiple comparisons
 197 according to Benjamini and Hochberg (false discovery rate 5%) and autodetection for log-
 198 transformation. The dashed line indicates an adjusted *P* value of 0.05.



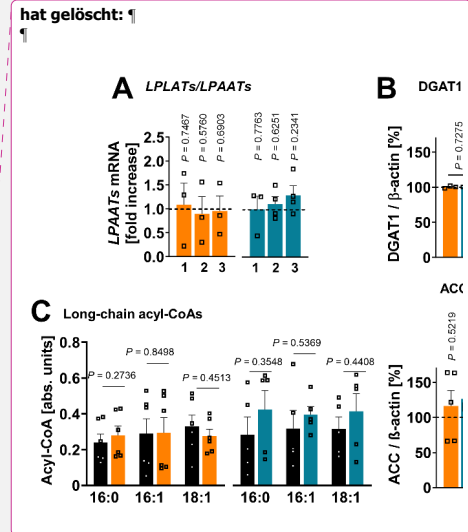
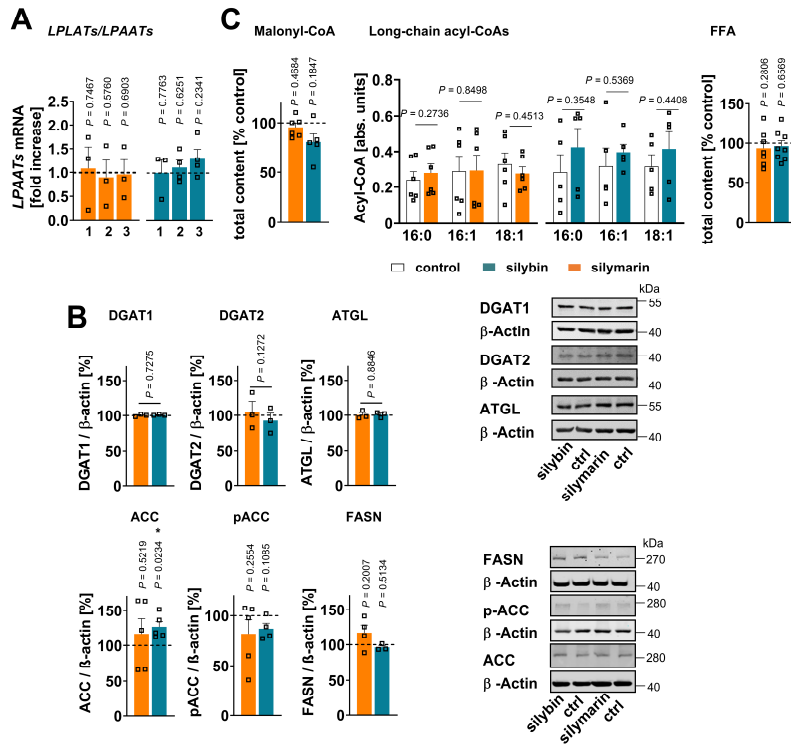
200

201 Figure S11. Lipid metabolic enzymes differentially regulated by silymarin/silybin. Comparative
 202 analysis of transcriptome data from silymarin-treated HepG2 and Huh7.5.1 hepatocarcinoma cells,
 203 silybin- and silymarin-treated CaCo-2 colon carcinoma cells, and hepatocytes derived from HCV-
 204 infected mice receiving silybin. Radar plots indicating the fold change in *PLA2G6*, *MBOAT2*, *PLD1*,
 205 *DGAT2*, *LPIN2*, *PNPLA3*, *HSD17B1*, *MVK*, *CYP4F2*, *HADH*, *ACOX2*, and *CYP2C19* expression by
 206 silymarin (HepG2, Huh7.5.1, CaCo-2) or silybin (hepatocytes, CaCo-2) relative to vehicle control.
 207 Non-adjusted *P* values given vs. vehicle control; multiple two-tailed unpaired Student's *t*-tests. Data
 208 are identical to [Figure 4](#).

209

210

hat gelöscht: Figure 6



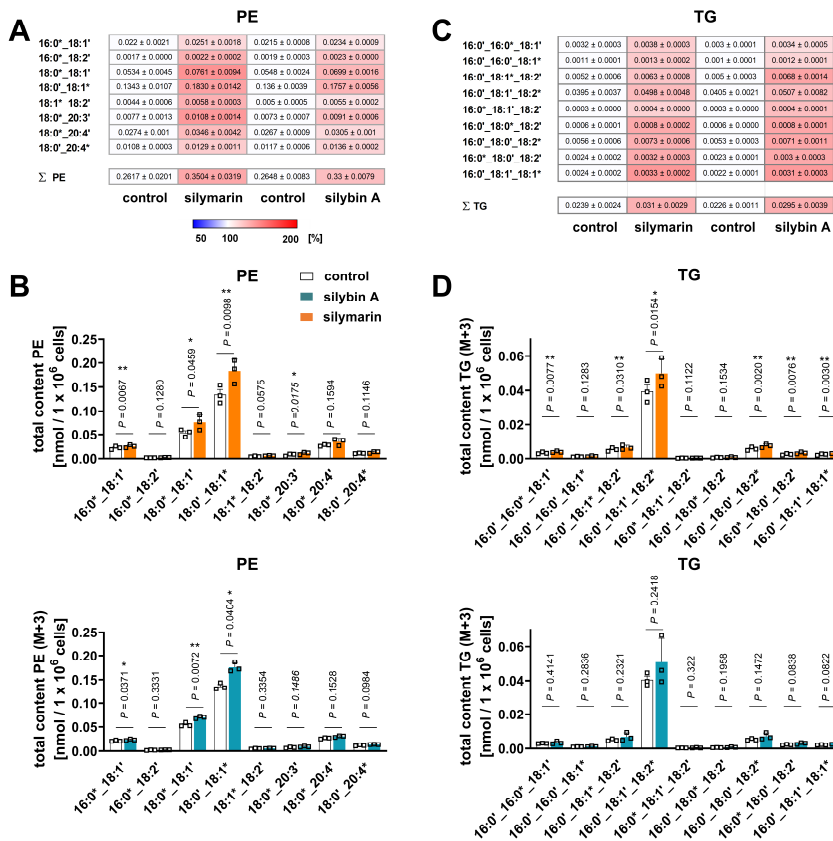
212
213 Figure S12. Remodeling of *de novo* phospholipid biosynthesis and TG metabolism. (A-C) HepG2
214 cells were incubated with silymarin (10 μ g/ml), silybin (20 μ M) or vehicle (ethanol for silymarin,
215 DMSO for silybin) for 24 h; (A) mRNA levels of *LPLAT/LPAAT1-3* normalized to β -actin
216 (*LPLATs/LPAATs* silybin) or *GAPDH* (*LPLATs/LPAATs* silymarin). Individual values and mean +
217 SEM as fold-change of control; $n = 3$ (*LPLATs/LPAATs* silymarin, *LPLAT1/LPAAT1* silybin) and n
218 = 4 (*LPLATs/LPAATs* silybin except *LPLAT1/LPAAT1*). (B) Protein expression of DGAT1, DGAT2,
219 ATGL/PNPLA2, ACC1/2 and FASN, phosphorylation of ACC1/2. Individual values and mean +
220 SEM; $n = 3$ (DGAT1, DGAT2, ATGL, FASN silybin), $n = 4$ (pACC silybin, FASN silymarin), and n
221 = 5 (ACC, pACC silymarin). Individual values and mean + SEM; $n = 3$. Representative Western blots
222 are shown. (C) Effects of silymarin and silybin on the cellular content of malonyl-CoA, long-chain
223 acyl-CoAs (normalized to the internal standard [13 C]-malonyl-CoA) and FFAs. Individual values and
224 mean + SEM; $n = 5$ (silybin, malonyl-CoA and long-chain acyl-CoAs) and $n = 6$ (silymarin, malonyl-
225 CoA and long-chain acyl-CoAs), $n = 7$ (silymarin, FFA) or $n = 8$ (silybin, FFA). * $P < 0.05$ vs. vehicle
226 controls; two-tailed paired Student's *t*-tests.

hat gelöscht: on the cellular ratio of

hat gelöscht: ,

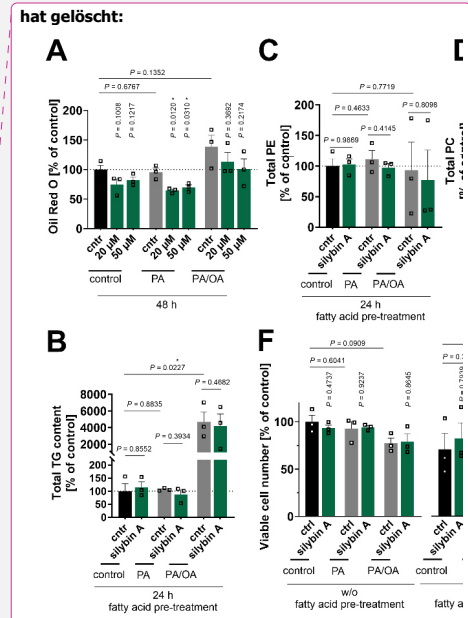
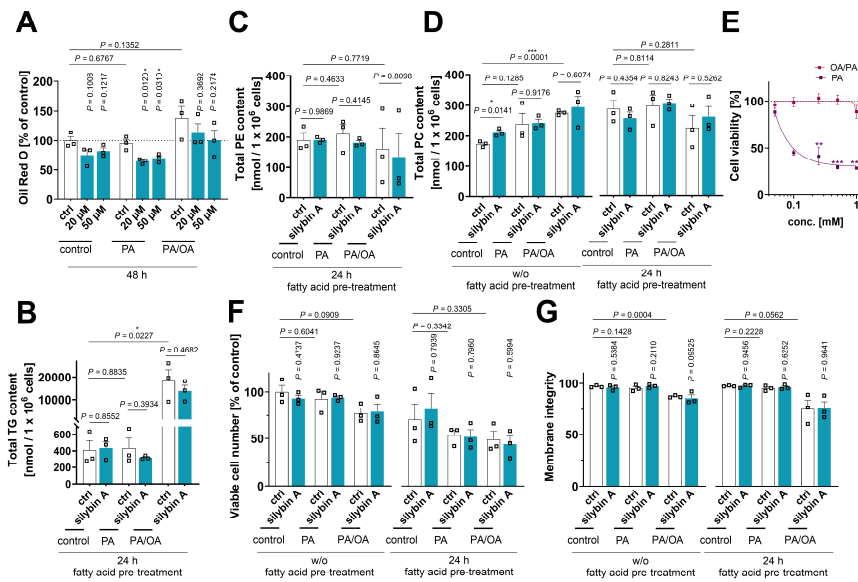
227

228



hat formatiert: Englisch (Vereinigtes Königreich)

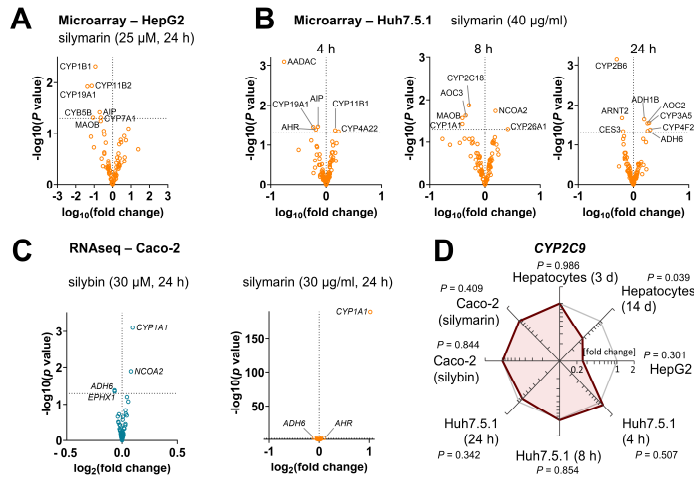
235
 236 **Figure S13. Incorporation of sodium acetate-¹³C₂, d₃ into phospholipid and TG species of human**
 237 **HepG2 cells treated with silymarin or silybin A. (A-D) Human HepG2 cells were treated as described**
 238 **in Figure 4I and J. (A, B) The heatmap and bar charts display the absolute amount of isotopically-**
 239 **labeled PE species, corrected for naturally occurring isotopes and normalized to internal standard and**
 240 **cell number in nmol / 1 × 10⁶ cells, as mean ± SEM, with color indicating percentage changes to the**
 241 **vehicle control. Data and the number of experiments are identical to Figure 4I. (C, D) The heatmap**
 242 **and bar charts display the absolute amounts of isotopically labeled TG species, corrected for naturally**
 243 **occurring isotopes and normalized to the internal standard and cell count in nmol / 1 × 10⁶ cells. Data**
 244 **are presented as mean ± SEM. The colors represent percentage changes relative to the vehicle control.**
 245 **Data and the number of experiments are identical to Figure 4J. Fatty acids that incorporated**
 246 **isotopically labeled sodium acetate (M+3) are indicated with asterisks (*) and fatty acids that remained**
 247 **in the molecule after fragmentation are indicated with primes ('). (B, D) Individual values and means ±**
 248 **SEM; n = 3. *P < 0.05, **P < 0.001 vs. vehicle controls; two-tailed paired Student's *t*-tests.**



249

250 Figure S14. Comparison of the silybin A effects in non-challenged hepatocytes and cell-based disease
 251 models of MAFLD and acute lipotoxicity. (A) HepaRG cells were treated with 0.1 mM palmitate (PA)
 252 or a mixture of PA/oleate (OA) in a 1:2 ratio (in total 1 mM) together with vehicle (DMSO, 0.5%) or
 253 compounds for 48 h. Relative lipid droplet content was determined by Oil Red O staining. (B-D)
 254 HepaRG cells were either pre-treated with 0.1 mM palmitate (PA) or a mixture of PA/oleate (OA) in a
 255 1:2 ratio (in total 1 mM) for 24 h followed by vehicle (DMSO, 0.5%) or silybin A (20 μ M) treatment
 256 or cells were directly co-treated with vehicle (DMSO, 0.5%) or silybin A (20 μ M), and the incubation
 257 was prolonged for a further 24 h. Total levels of TG (B), PE (C), and PC (D) determined by UPLC-
 258 MS/MS. (E) Cell viability measured by MTT assay. (F) Viable cell numbers. (G) Cell membrane
 259 integrity determined by trypan blue staining. Individual values and mean \pm SEM or \pm SEM, $n = 2$ (E,
 260 0.1 mM PA) or $n = 3$ (A-G, except D, 0.1 mM PA). * $P < 0.05$, *** $P < 0.001$ vs. control; two-tailed
 261 unpaired Student's t -test.

hat gelöscht: 3

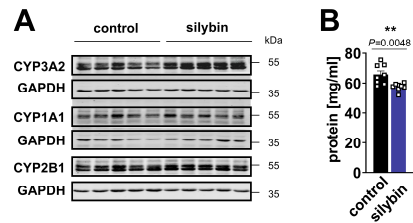


265

266 Figure S15. Silymarin/silybin kinetically controls the mRNA levels of genes involved in drug
 267 metabolism. Comparative analysis of transcriptome data from silymarin-treated HepG2 and Huh7.5.1
 268 hepatocarcinoma cells, silybin- and silymarin-treated CaCo-2 colon carcinoma cells, and hepatocytes
 269 derived from HCV-infected mice receiving silybin. (A-C) Volcano plots compare the expression of
 270 proteins involved in drug metabolism upon silymarin (A-C) or silybin (C) treatment vs. vehicle
 271 control. Statistical calculations were performed by pairwise comparison of treatment and control
 272 groups using the GEO2R interactive webtool (<https://www.ncbi.nlm.nih.gov/geo/geo2r/>)¹. *P*-values
 273 were calculated by multiple *t*-tests without correction for multiple comparisons. The dashed line
 274 indicates a *P*-value of 0.05. (D) Radar plots indicating the fold change in *CYP2C9* by silymarin
 275 (HepG2, Huh7.5.1, CaCo-2) or silybin (hepatocytes, CaCo-2) relative to vehicle control. Non-adjusted
 276 *P* values are given vs. vehicle control; multiple two-tailed unpaired Student's *t*-tests.

277

hat gelöscht: 4



279

280 Figure S16. Impact of silybin on CYP expression in mouse liver. (A) Western blots for the
 281 densitometric data shown in Figure 8C are representative of $n = 5$ mice/group; (B) Protein
 282 concentration of the $9,000\times g$ supernatant of the liver homogenate. Individual values and mean + SEM;
 283 $n = 8$ mice/group. $**P < 0.01$ vs. vehicle control; two-tailed unpaired Student's t -test.
 284

285

hat gelöscht: 5

287 Supplementary Notes

288 Supplementary Note 1: Cholesterol and CE metabolism

289 The effects of silybin/silymarin on CEs, the second major neutral lipid in lipid droplets after
 290 TGs, are less consistent. In some settings, silybin/silymarin stimulates cholesterol
 291 biosynthesis by upregulating the transcription factor *SREBP1* (Figure 4A) and repressing its
 292 endoplasmic reticulum anchor *INSIG1* (Figure 4D and E), thereby favoring the transfer of
 293 *SREBP1* to the Golgi for proteolytic procession to the mature form²⁻⁴. On the contrary, several
 294 SREBP-regulated target genes were downregulated (*ACACA*, *ELOVL6*, *MVK*, Figure 4A, E,
 295 Figure S11), except for *FASN*, which was upregulated as expected (Figure 4C). In other
 296 settings, silybin/silymarin reduces the expression of cholesterol biosynthetic enzymes (*MVK*,
 297 *TM7SF2*, Figure 4C, D, and E, and Figure 11). Such counter-regulation could be explained by
 298 initially increased levels of sterols, which then bind to the cholesterol sensor *INSIG1* (Figure
 299 S6 D and E) and suppress SREBP1 signaling (along with target protein expression) without
 300 necessarily interfering with SREBP1 expression². In addition to canonical cholesterol
 301 biosynthesis, increased lipoprotein and sterol uptake (*LRP2*) (Figure 4B and C) and possibly
 302 endosomal cholesterol transport (*STARD3NL*) (Figure 4C) may further add to the
 303 accumulation of intracellular CE. In strong support of this hypothesis, silymarin
 304 administration to mice substantially elevated the hepatic CE content (Figure 1D). However,
 305 the increase in esterified cholesterol levels did not seem to be translated into enhanced
 306 cholesterol metabolism, as the expression of various sterol-metabolizing enzymes (*CYP11A1*,
 307 *CYP11B1*, *CYP2C8*, *CYP3A4*, *CYP7A1*, *CYP11B2*, *CYP17A1*, *CYP19A1*, *CYP27A1*, *ABCB11*,
 308 *SLC10A1*, *SLC27A5*, *HSD3B2*, *HSD17B1*, *HSD17B3*, *AKR1D1*, *AKR1C3*, *EBP*, *BAAT*, *STS*)
 309 is largely repressed (Figure 4A, B, C, D and E, and Figure S11), with a few exceptions
 310 (*CYP11A1*, *CYP11B1*, *CYP11B2*, *AKR1C3*, Figure 4B-D). Together, silymarin/silybin
 311 consistently downregulate anabolic and catabolic sterol metabolism, while exerting complex,
 312 partially opposite effects on cholesterol biosynthesis.

313 Supplementary Note 2: Vitamin A metabolism

314 In addition, silymarin/silybin differentially regulates a significant number of genes related to
 315 vitamin A metabolism, including retinoic acid biosynthesis (*CYP11B1*, *CYP3A4*, *ADH1B*,
 316 *ADH6*, Figure 4A, Figure S14A-C), degradation (*CYP2C18*, *CYP3A5*, *CYP26A1*, *CYP2C8*,
 317 Figure 8A and B, Figure S14B), and vitamin A storage (*DGAT1*, *PNPLA3* and *ATGL*/
 318 *PNPLA2*, Figure 4A, B, E, and F, Figure S11).

hat gelöscht: Figure 6

hat gelöscht: Figure 6

hat gelöscht: Figure 6

hat gelöscht: Figure 6

hat gelöscht: Figure 6

hat gelöscht: Figure 6

hat gelöscht: Figure 6

hat gelöscht: Figure 6

hat gelöscht: Figure 6

hat gelöscht: 8

hat gelöscht: Figure 6

330 Vitamin A is stored as retinyl esters in lipid droplets in the liver and shares common
 331 metabolic pathways with TG. This involves genetic risk factors for MAFLD, such as *DGATI*,
 332 *PNPLA3*, and *ATGL/PNPLA2*, which participate in retinol ester synthesis and degradation^{5,6}.
 333 Vitamin A plays a central role in the regulation of hepatic lipid metabolism, including
 334 lipogenesis, lipid transport, and lipid catabolism⁶, and disturbed vitamin A metabolism has
 335 been associated with MAFLD^{5,6}. It is therefore remarkable that our comparative transcriptome
 336 analysis revealed that numerous genes involved in vitamin A metabolism (including *CYP11B1*,
 337 *CYP3A4*, *ADH1B*, *ADH6*, *CYP2C18*, *CYP3A5*, *CYP26A1*, *CYP2C8*, *DGATI*, *PNPLA2/ATGL*
 338 and possibly *PNPLA3*) are subject to regulation by silybin/silymarin. Further studies are
 339 needed to explore whether the interference with vitamin A metabolism by silymarin/silybin
 340 affects hepatic lipid metabolism and influences the development and/or progression of
 341 MAFLD.

hat gelöscht: s

hat gelöscht: s

hat gelöscht: s

343 References

- 344 1 Barrett, T. *et al.* NCBI GEO: archive for functional genomics data sets--update.
 345 *Nucleic Acids Res* **41**, D991-995, doi:10.1093/nar/gks1193 (2013).
 346 2 Yang, T. *et al.* Crucial step in cholesterol homeostasis: sterols promote binding of
 347 SCAP to INSIG-1, a membrane protein that facilitates retention of SREBPs in ER.
 348 *Cell* **110**, 489-500, doi:10.1016/s0092-8674(02)00872-3 (2002).
 349 3 Engelking, L. J., Cantoria, M. J., Xu, Y. & Liang, G. Developmental and extrahepatic
 350 physiological functions of SREBP pathway genes in mice. *Semin Cell Dev Biol* **81**,
 351 98-109, doi:10.1016/j.semcdb.2017.07.011 (2018).
 352 4 Chen, Y. *et al.* Maturation and activity of sterol regulatory element binding protein 1
 353 is inhibited by acyl-CoA binding domain containing 3. *PLoS One* **7**, e49906,
 354 doi:10.1371/journal.pone.0049906 (2012).
 355 5 Saeed, A. *et al.* Impaired Hepatic Vitamin A Metabolism in NAFLD Mice Leading to
 356 Vitamin A Accumulation in Hepatocytes. *Cell Mol Gastroenterol Hepatol* **11**, 309-
 357 325 e303, doi:10.1016/j.jcmgh.2020.07.006 (2021).
 358 6 Saeed, A., Dullaart, R. P. F., Schreuder, T., Blokzijl, H. & Faber, K. N. Disturbed
 359 Vitamin A Metabolism in Non-Alcoholic Fatty Liver Disease (NAFLD). *Nutrients* **10**,
 360 doi:10.3390/nu10010029 (2017).
 361

hat formatiert: Französisch (Frankreich)

hat formatiert: Französisch (Frankreich)

362

363

364